

# The Tibetan Plateau's Far-Reaching Impacts on Arctic and Antarctic Climate: Seasonality and Pathways

LIPING WANG,<sup>a</sup> HAIJUN YANG,<sup>b,c</sup> QIN WEN,<sup>d</sup> YIMIN LIU,<sup>e,f</sup> AND GUOXIONG WU<sup>e,f</sup>

<sup>a</sup> Department of Atmospheric and Oceanic Sciences, School of Physics, Peking University, Beijing, China

<sup>b</sup> Department of Atmospheric and Oceanic Sciences and CMA-FDU Joint Laboratory of Marine Meteorology, Fudan University, Shanghai, China

<sup>c</sup> Shanghai Scientific Frontier Base for Ocean–Atmosphere Interaction Studies, Fudan University, Shanghai, China

<sup>d</sup> School of Geography, Nanjing Normal University, Nanjing, China

<sup>e</sup> State Key Laboratory of Numerical Modelling for Atmospheric Sciences and Geophysical Fluid Dynamics, Institute of Atmospheric Physics, Chinese Academy of Sciences, Beijing, China

<sup>f</sup> College of Earth Science, University of Chinese Academy of Sciences, Beijing, China

(Manuscript received 19 March 2022, in final form 23 October 2022)

**ABSTRACT:** As the highest and most extensive plateau in the world, the Tibetan Plateau (TP) has remarkable effects on global climate. Through coupled model sensitivity experiments with and without the TP, we show that the TP can affect the Arctic directly via orography-forced stationary waves, and influence the Antarctic indirectly via stationary waves forced by sea surface temperature (SST) in the Indian Ocean. These far-reaching impacts occur mainly in wintertime. The fast atmospheric processes play an important role; particularly, the midlatitude westerly flow, which is stronger and closer to the equator in winter, provides a favorable condition for the eastward and poleward energy propagation of the forced waves. In the Northern Hemisphere, removing the TP causes a wave train traveling from the Asian continent to the North America–Atlantic Ocean region, resulting in intensified westerlies and thus an enhancement of stratospheric polar vortex and Arctic cooling. The pathways are northeastward directly in the upper level due to the background westerlies, while they are eastward and then northeastward in the lower level, modulated by the winter monsoon. To the south, the TP perturbation causes an anomalous cross-equatorial flow, leading to an anomalous SST dipole pattern in the Indian Ocean in the austral winter; this generates stationary waves propagating energy southeastward from the tropical Indian Ocean to the Antarctic, resulting in a Rossby wave train circulating around the Antarctic. Our study identifies the seasonality and pathways of the TP affecting the polar regions, which may help to understand the role of the TP in the future climate changes in polar regions.


**KEYWORDS:** Antarctica; Arctic; Planetary waves; Atmosphere–ocean interaction

## 1. Introduction

As the highest and most extensive plateau in the world, the Tibetan Plateau (TP) has played a crucial role in shaping Earth's climate (e.g., Yeh 1957; Yeh and Gao 1979; Yanai et al. 1992; Yanai and Wu 2006; Cheng and Wu 2007; Wu et al. 2007, 2012a,b; Duan and Wu 2008; Yao et al. 2012). Paleoclimatic evidence suggests the uplift of the TP can be traced back to approximately 50 Ma (million years ago); it was accelerated about 10–8 Ma (Harrison et al. 1992; Molnar et al. 1993). This uplift is thought to have promoted the evolution of Asian monsoon climate and central Asian aridity (Ramstein et al. 1997; An et al. 2001). Paleoclimatic evidence and model results also suggest that the TP may have contributed to the formations of polar ice caps (Raymo et al. 1988; Ruddiman and Kutzbach 1989; Raymo and Ruddiman 1992) and global thermohaline circulations, particularly the formation of the Atlantic meridional overturning

circulation (AMOC) (Su et al. 2018; Wen and Yang 2020; Yang and Wen 2020).

The TP exerts remarkable influences on regional and global climate through its thermal and mechanical effects (e.g., Kutzbach et al. 1989; Liu and Yin 2002; Wu et al. 2007, 2015; Boos and Kuang 2010; Molnar et al. 2010). In summer, the TP acts as a strong heat engine that enhances the Asian monsoon, in particular its associated precipitation (Kutzbach et al. 1989; Hsu and Liu 2003; Duan and Wu 2005). Such heating effect drives a cyclonic circulation in the lower troposphere, pumping the warm and moist air from the surrounding surface areas to the upper troposphere. The thermal effect is thought to be dominant in the boreal summer. In winter, its mechanical effect is more important because of the strong impinging flows upon the TP (Duan and Wu 2005; Wu et al. 2012a,b). The winter westerlies impinging upon the orography can generate an “asymmetric dipole” pattern, with a large-scale anticyclonic (cyclonic) circulation upstream (downstream) in the upper level, and a large anticyclonic (cyclonic) circulation to the north (south) in the lower

 Denotes content that is immediately available upon publication as open access.

Corresponding author: Haijun Yang, yanghj@fudan.edu.cn



This article is licensed under a [Creative Commons Attribution 4.0 license](http://creativecommons.org/licenses/by/4.0/) (<http://creativecommons.org/licenses/by/4.0/>).

DOI: 10.1175/JCLI-D-22-0175.1

© 2023 American Meteorological Society. For information regarding reuse of this content and general copyright information, consult the [AMS Copyright Policy](https://www.ametsoc.org/PUBSReuseLicenses) ([www.ametsoc.org/PUBSReuseLicenses](https://www.ametsoc.org/PUBSReuseLicenses)).

level, which intensifies the winter cold break from Siberia (Wu et al. 2007). Previous studies have emphasized the role of the TP in the Asia–Pacific climate, whereas its remote impact, especially on the Arctic and the Antarctic, is rarely mentioned.

Polar regions are significant parts of the climate system, and have intense feedbacks on the global climate via strong coupling between ice sheets, atmosphere, and surrounding seas (Budikova 2009; Vihma 2014). Paleoclimatic evidence suggests that the climate in the Arctic and the Antarctic has undergone tremendous changes since the Cenozoic. Antarctic glaciation may have started around 43 Ma, and then expanded in the early Oligocene around 34 Ma (Miller et al. 1987; Zachos et al. 2001). Arctic ice appeared since the late Miocene of  $\sim 10$ –6 Ma (Lear et al. 2000) because of the bipolar cooling events during the Cenozoic. The timing was close to that of the TP uplift. Model results showed that the global cooling in the Cenozoic may have been caused by the uplift of the TP, which promoted an increase in chemical weathering rate, lowering the concentration of atmospheric  $\text{CO}_2$  and thus leading to the growth of large ice sheets in both hemispheres and of polar ice caps (Raymo et al. 1988; Ruddiman and Kutzbach 1989; Raymo and Ruddiman 1992). Therefore, the role of the TP on polar regions deserves an in-depth investigation.

This study focuses on how and to what extent the TP can affect the polar regions, using a fully coupled climate model of CESM1.0. We attempt to answer the following questions: What are the pathways of the TP's influence? In which season is the teleconnection robust? By comparing the sensitivity experiments with and without the TP, we demonstrate that the TP can affect the Arctic directly by TP-forced stationary waves, and the Antarctic indirectly via the stationary waves forced by anomalous sea surface temperature (SST) in the tropical Indian Ocean. Atmospheric processes play important roles. Removing the TP leads to an enhancement of the westerlies in the Northern Hemisphere (NH) and a deepening of the stratospheric polar vortex that cools the Arctic in the upper troposphere and lower stratosphere. The warming over the TP region and the large-scale southwesterly wind induce warm poleward advection, which warms up the Arctic in the lower level. Removing the TP also causes a weakening of the westerlies in the Southern Hemisphere (SH) and temperature changes around the Antarctic via stationary waves generated over the Indo-Pacific oceans. The background westerlies in the midlatitudes determine that it is in the boreal (austral) winter that the perturbation over the TP can affect the Arctic (Antarctic) most.

This paper is organized as follows. An introduction to the model and experiments is given in section 2. The TP's effects on the Arctic and Antarctic are demonstrated in sections 3 and 4, respectively. A summary and discussion are given in section 5.

## 2. Model and experiments

The model used in this study is the Community Earth System Model (CESM1.0) of the National Center for Atmospheric Research (NCAR). The CESM1.0 is a fully coupled global climate model that provides state-of-the-art simulations of Earth's past, present, and future climate states (<http://www2.cesm.ucar.edu/>). CESM is composed of an atmosphere model

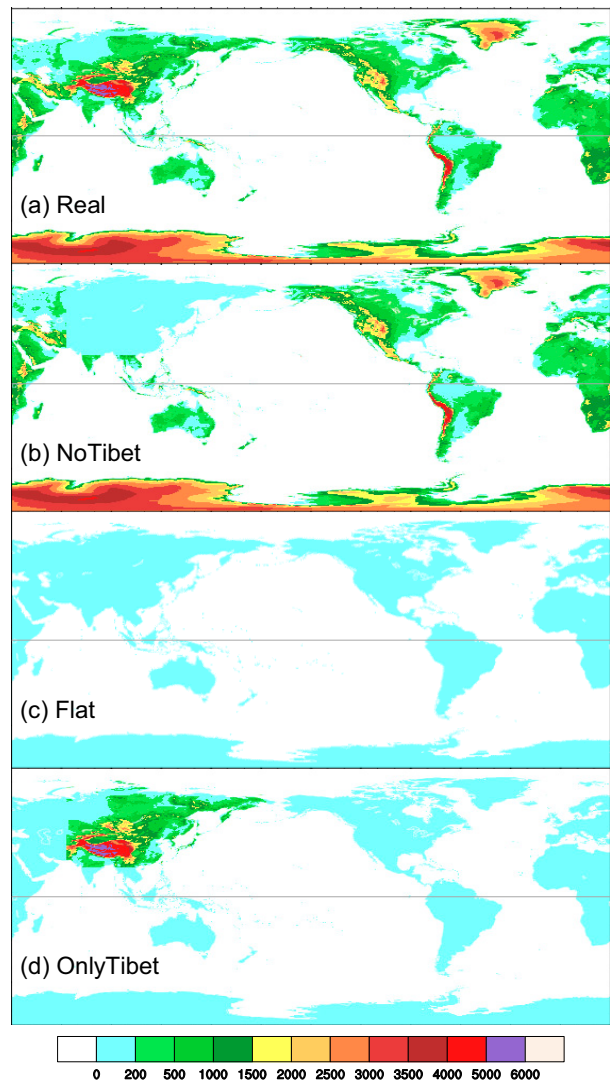


FIG. 1. Topography configuration in coupled model experiments. (a) Realistic topography used in Real (the control run), (b) modified topography without the Tibetan Plateau (TP) used in NoTibet, (c) modified topography with flat global topography used in Flat, and (d) modified topography with only TP topography used in OnlyTibet. Here high-resolution topography data with horizontal resolution of  $0.17^\circ \times 0.17^\circ$  are used to plot this figure.

(Community Atmosphere Model; CAM4) (Park et al. 2014), land surface model (Community Land Model; CLM4) (Lawrence et al. 2012), ocean model (Parallel Ocean Program; POP2) (Smith et al. 2010), sea ice model (Community Ice Code; CICE4) (Hunke and Lipscomb 2010), and one coupler (CPL7). The CAM4 uses the grid T31\_gx3v7, with the horizontal resolution of about  $3.75^\circ \times 3.75^\circ$  and 26 vertical levels. The CLM4 has the same horizontal resolution as the CAM4. The POP2 has 60 vertical levels, and a uniform  $3.6^\circ$  spacing in the zonal direction. In the meridional direction, the grid is nonuniformly spaced: it is  $0.6^\circ$  near the equator, gradually increases to the maximum  $3.4^\circ$  at

TABLE 1. List of the experiments used in this study.

Model	Experiment	Description
Fully coupled	Real	2400-yr control run with realistic topography
	NoTibet	400-yr run with TP topography removed, starting from year 2001 of Real
	Flat	1200-yr control run with flat global topography
	OnlyTibet	400-yr run with real TP topography, starting from year 801 of Flat
AGCM	Real_SST	30-yr run forced by the global SST from Real climatology with seasonal cycle
	NoTibet_SST	30-yr run forced by the global SST from NoTibet climatology with seasonal cycle
	NoTibet_TroSST	SST in tropical oceans (20°S–20°N) from NoTibet; SST in the other regions from Real
	NoTibet_TroIO	SST in tropical Indian Ocean (20°S–20°N, 50°–160°E) from NoTibet; SST in the other regions from Real
	NoTibet_TroPac	SST in tropical Pacific (20°S–20°N, 160°E–80°W) from NoTibet; SST in the other regions from Real
	NoTibet_TroAtl	SST in tropical Atlantic (20°S–20°N, 80°W–20°E) from NoTibet; SST in the other regions from Real
	NoTibet_TroIO_1.5	SST in 20°S–20°N, 50°–160°E set to 1.5°C
	NoTibet_TroIOPac_1.5	SST in 20°S–20°N, 50°E–90°W set to 1.5°C

35°N/S, and then decreases poleward. The CICE4 has the same horizontal grid as the POP2. No flux adjustments are used in CESM1.0.

Two groups of experiments with different orography were carried out (Fig. 1). The first group includes a 2400-yr control run and a 400-yr sensitivity experiment without the TP orography. The control run (named “Real”) has realistic geometry, orography, and continents in the model (Yang et al. 2015) (Fig. 1a). The sensitivity experiment (named “NoTibet”) starts from year 2001 of Real and is integrated for 400 years, with the orography around the TP set to 50 m above the mean sea level (Fig. 1b). The second group includes a 1200-yr control run with a global flat continent (named “Flat”) and a 400-yr sensitivity experiment with only the TP available (named “OnlyTibet”). In Flat, the global orography is reset as 50 m above mean sea level (Fig. 1c). OnlyTibet is similar to Flat, except that the TP region has realistic orography, and it starts from year 801 of Flat and is integrated for 400 years (Fig. 1d). All conditions except for the TP orography in these experiments comply with the standard configuration and a preindustrial CO<sub>2</sub> level of 285 ppm. These experiments are single orography sensitivity tests, rather than paleoclimate simulation experiments in which one should prescribe several geologic boundary conditions simultaneously.

The responses of the Arctic and Antarctic to the TP removal are obtained by subtracting the results of Real from those of NoTibet (NoTibet minus Real). For comparison, the responses due to the TP presence are obtained by subtracting the results of Flat from those of OnlyTibet (OnlyTibet minus Flat). Since the responses of the Arctic and Antarctic to TP removal are opposite to those with TP presence and they have roughly the same magnitude, we focus on the results from NoTibet and Real in the following sections. We investigate the seasonality and pathways of the TP affecting the polar regions. The boreal winter (austral summer) is December–February (DJF), and the boreal summer (austral winter) is June–August (JJA).

We performed six atmospheric general circulation model (AGCM) experiments using the CAM4 of CESM1.0 to further investigate the influence of the TP on the Antarctic via atmospheric pathway. The atmospheric model is driven by prescribed SSTs obtained from Real or NoTibet. All the AGCM experiments have the real-world orography. The global SST experiments, named Real\_SST and NoTibet\_SST, are forced by the prescribed global SST from the mean seasonal cycle of Real and NoTibet, respectively. The tropical SST experiment, named NoTibet\_TroSST, is forced by the prescribed tropical SST from NoTibet. Outside the tropics, the SST is prescribed as in Real. Three regional tropical SST experiments, named NoTibet\_TroIO, NoTibet\_TroPac, and NoTibet\_TroAtl, are similar to NoTibet\_TroSST, except that they are forced by prescribed tropical Indian Ocean SST, tropical Pacific SST, and tropical Atlantic SST, respectively. We performed another two experiments to examine the effects of size and sign of forcing on the Rossby wave train in the SH. These two experiments, named NoTibet\_TroIO\_1.5, NoTibet\_TroIOPac\_1.5, are forced by the prescribed SST in the tropical Indian Ocean and Indian–Pacific Ocean, respectively. More details on the regions of the tropical forcing are listed in Table 1.

All these AGCM experiments are integrated for 30 years each, starting from year 2001 of Real. The changes are obtained by subtracting the results of Real\_SST from each sensitivity experiment. The averaged changes over years 1–30 are used for analysis. We use Student’s *t* test to examine the statistical significance of our results. We found that most changes are significant at the 95% confidence level, which is expected because altering the TP topography induces strong mechanical forcing and strong responses around the globe.

### 3. From the Tibetan Plateau to the Arctic

#### a. Transient changes in the Northern Hemisphere

In response to the TP removal, a significant cooling occurs in the upper troposphere and stratosphere in the Arctic

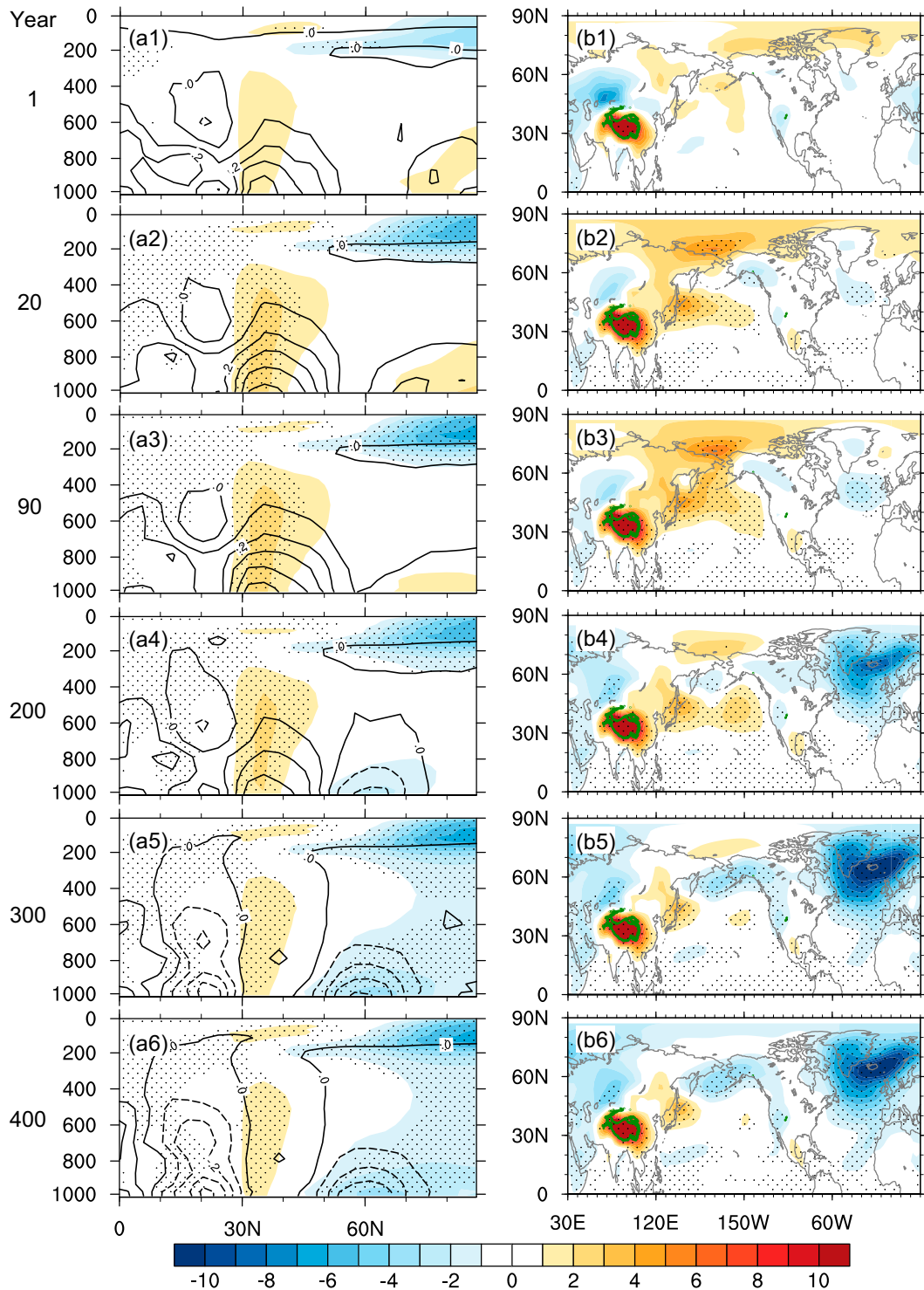


FIG. 2. Pressure–latitude section showing changes in (left) zonal mean air temperature (shading;  $^{\circ}\text{C}$ ) and specific humidity (contours;  $\text{g kg}^{-1}$ ), and (right) surface air temperature (SAT;  $^{\circ}\text{C}$ ) in NoTibet with respect to Real. (from top to bottom) The changes are averaged over year 1 and years 15–25, 85–95, 190–210, 290–310, and 380–400. Stippling represents the temperature changes are significant at the 95% confidence level based on Student's  $t$  test.



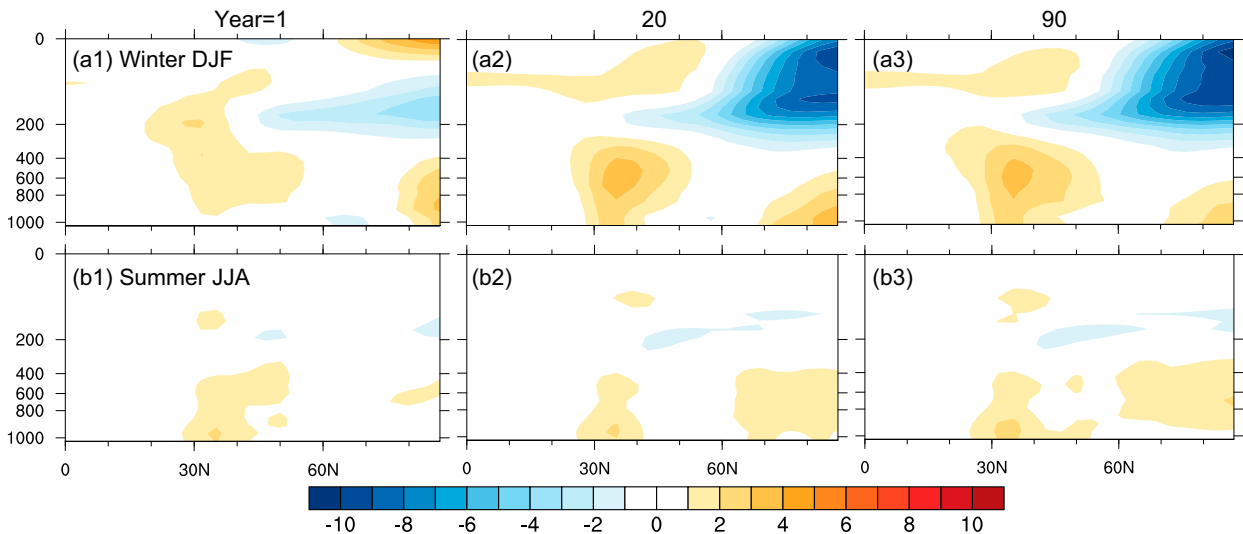


FIG. 3. Pressure–latitude section showing changes in zonal mean air temperature (shading; °C) in (top) boreal winter and (bottom) boreal summer in NoTibet with respect to Real. (from left to right) The changes are averaged over year 1, years 15–25, and years 85–95.

(Fig. 2a). This cooling appears immediately after the TP removal (Fig. 2a1), reaches the maximum strength in about 20 years (Fig. 2a2), and remains steady thereafter (Figs. 2a3–a6), suggesting the atmospheric processes reach quasi-equilibrium state quickly. Figure 2a implies a robust pathway and mechanism that can convey the perturbation swiftly and efficiently from the TP to the Arctic. The seasonality, pathways, and mechanism of the TP affecting the Arctic through *atmospheric processes* are the foci in this subsection.

In response to the TP removal, the NH in general becomes warmer and wetter in the first several decades due to atmospheric processes (Figs. 2a1–a3); it then becomes colder and drier due to ocean processes (Figs. 2a4–a6), that is, the slowdown and final shutdown of the AMOC, which was reported for these same experiments in detail in Yang and Wen (2020). Fast response (the first 100 years) is the focus in this paper, which results mainly from atmospheric processes, as the ocean has yet to adjust. When the TP is removed, there is immediately a strong surface warming over the TP region (Fig. 2b1), resulting mainly from the lapse rate effect in the troposphere. The changes of atmospheric zonal mean temperature around the TP are roughly barotropic (Fig. 2a1). In the first 100 years, the lower-level subpolar and Arctic regions become warmer because of a large-scale poleward heat transport from the TP region (Figs. 2b1–b3). The surface cooling over the Arctic in the later stage (Figs. 2a4 and 2b4) is mainly caused by the ocean dynamics. The upper-level cooling over the Arctic is mainly related to the atmosphere dynamics. Two different dynamics lead to a significant baroclinic response in the atmosphere over the Arctic. Through this sensitivity experiment, we demonstrate that the climate perturbation over the TP has a quick and strong influence on the Arctic. Identifying the quick atmospheric processes will help us reveal the seasonality and pathways via which the TP affects the Arctic. In Fig. 2 most changes are significant at the 95% confidence level, suggesting the robust connection between the

TP and the Arctic. For visual clarity, we do not show significance test in other figures in this section.

It is in the boreal winter that the TP can really affect the Arctic (Fig. 3a). In the boreal summer, even the local change over the TP region is suppressed, and the remote response over the Arctic is negligible (Fig. 3b). In winter, the Arctic upper-level cooling appears first in the lower stratosphere; it becomes strong in the upper troposphere and the whole stratosphere in 100 years (Fig. 3a3). This strong winter cooling is mainly due to the deepening of the winter polar vortex (Fig. 4b). Figure 4b shows the wintertime intensified westerlies and cooling center in the polar region. The polar low is enhanced significantly in winter. The polar vortex refers to a planetary-scale westerly flow that encircles the pole in the mid-to-high latitudes (Vaugh et al. 2017). Removing the TP leads to intensified westerlies in mid-to-high latitudes in the upper level, suggesting the deepening of the polar vortex (a cyclonic geopotential height anomaly over the polar region in Fig. 4b), causing cooling in the Arctic. In summer, the upper-level atmospheric circulation is hardly changed over the Arctic (Fig. 4c). Here, we stress that the responses during the first 10 years (not shown) showed a resemblance to those during the first 100 years (Figs. 4 and 5), suggesting a quick adjustment of atmospheric circulation to the TP removal and the long-lasting effect of atmospheric processes.

The upper-level jet change can be seen more clearly in Fig. 5. The responses are roughly barotropic and significantly stronger in the stratosphere (Figs. 5a1,a2). The intensified westerly wind, accompanied by reduced meridional wind (not shown), suggesting an enhanced Northern Annular Mode (NAM; Ruddiman and Kutzbach 1989; Thompson et al. 2000; Thompson and Wallace 2001). The enhanced westerlies around 60°N indicate an enhancement of the stratospheric polar low (Matsuno 1971; Li and Wang 2003; Vaugh et al. 2017). The wintertime responses of zonal wind are similar to the annual mean results, but with much larger amplitude (Fig. 5a2). The westerlies

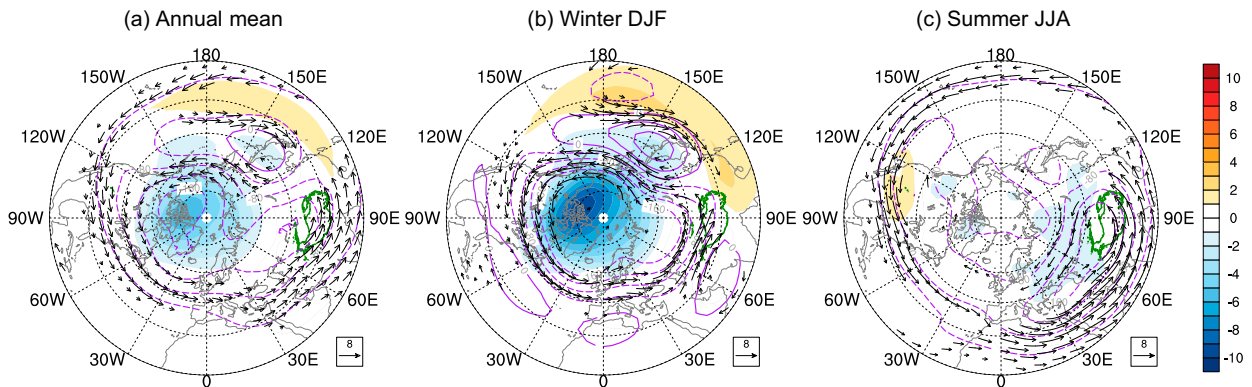


FIG. 4. Quasi-equilibrium changes in Northern Hemisphere atmosphere circulations averaged over 100–200 hPa in NoTibet with respect to Real for the (a) annual mean, (b) winter, and (c) summer, averaged over years 1–100. Contours represent geopotential height change (m), shading is for temperature change ( $^{\circ}\text{C}$ ), and vectors are for wind change ( $\text{m s}^{-1}$ ). The TP region is marked by the enclosed green contour. Vectors less than  $2 \text{ m s}^{-1}$  are omitted for clarity.

around  $30^{\circ}\text{N}$  become weaker because removing the TP weakens the subtropical jet stream on the eastern side of the orography (Manabe and Terpstra 1974). The summer-time responses are completely different because the NH westerlies have remarkable seasonal variation in both intensity and north–south displacement. In the boreal winter, the upper-level planetary westerlies shift southward and the TP is located directly at the path of the westerlies (Chiang et al. 2015). The TP acts as a huge barrier that can reduce the westerlies (Ruddiman and Kutzbach 1989; Wu et al. 2015). In contrast, the upper-level planetary westerlies shift northward and become weaker in the boreal summer. Therefore, only the northern edge of the TP lies in the path of the westerlies, while the remainder is in the easterlies. Removing

the TP causes warming over Asia at a lower altitude in the boreal summer (Fig. 3b), which induces an anomalous cyclone below the stratosphere (Fig. 4c), and thus weakens the westerlies (easterlies) in higher (lower) latitudes at a lower altitude of about 150 hPa (Fig. 5a3).

The perturbation of the TP can affect upward wave propagation, leading to changes in stratospheric wind and polar vortex. In the boreal winter, the background westerly wind (Fig. 5a2) in the stratosphere over the Arctic is favorable to the upward propagation of Eliassen–Palm flux (E-P flux; Eliassen and Palm 1960; Holton and Hakim 2013). Removing the TP reduces the upward wave propagation, with divergence of the E-P flux at the stratospheric vortex (Fig. 5b2), resulting in the enhancing westerly wind and polar vortex, and thus

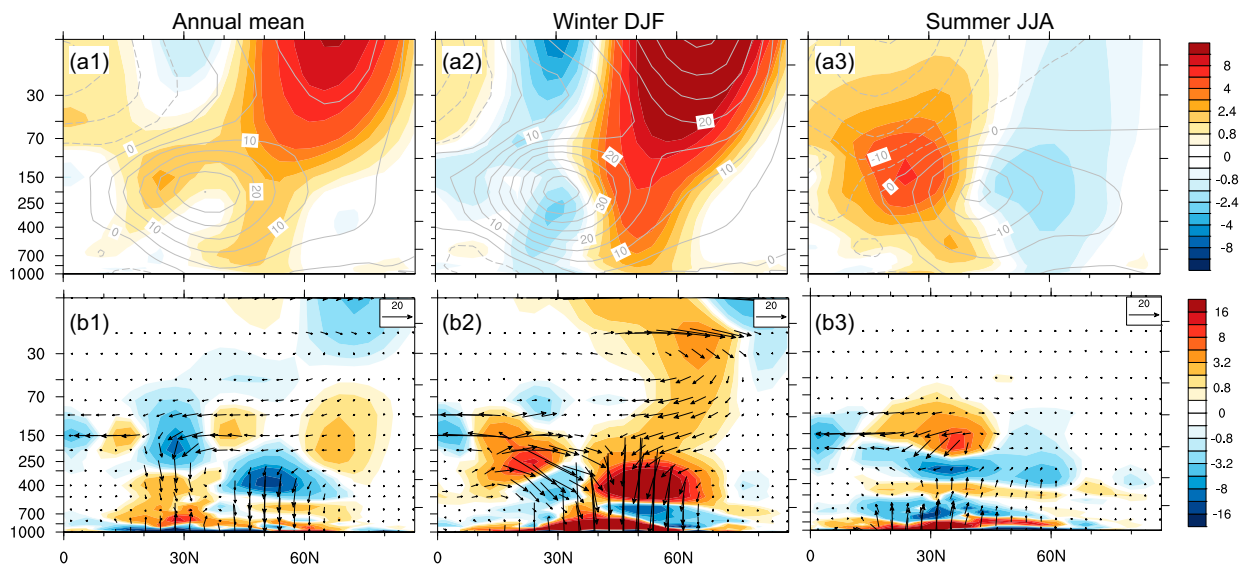


FIG. 5. Quasi-equilibrium changes in (top) zonal mean zonal wind (shading;  $\text{m s}^{-1}$ ) and (bottom) E-P flux (vectors;  $10^6 \text{ m}^2 \text{ s}^{-2}$ ) and its divergence (shading;  $\text{m s}^{-2}$ ) in NoTibet with respect to Real, averaged over years 1–100. Gray contours in (a) show the mean zonal wind in Real. Results are for the (a1),(b1) annual mean, (a2),(b2) boreal winter, and (a3),(b3) boreal summer. The E-P flux is multiplied by the square root of  $1000/\text{pressure}$  to aid visualization, while its divergence is not scaled.

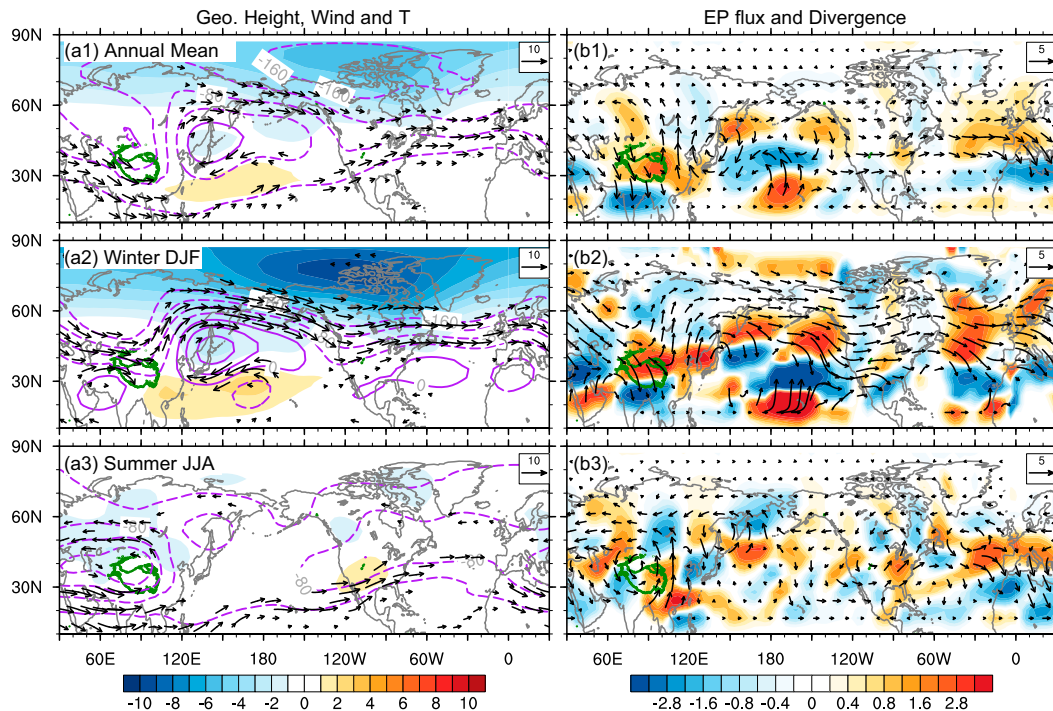


FIG. 6. (left) As in Fig. 4, but for the Mercator projection. (right) Quasi-equilibrium change in wave activity flux (vectors;  $\text{m}^2 \text{s}^{-2}$ ) and its divergence (shading;  $10^6 \text{m}^2 \text{s}^{-2}$ ) averaged over 100–200 hPa in NoTibet with respect to Real. Positive (negative) value represents divergence (convergence). Results are shown for the (top) annual mean, (middle) boreal winter, and (bottom) boreal summer. All these values are averaged over years 1–100. The TP region is marked by the enclosed green contour. Vectors less than  $2 \text{m s}^{-1}$  are omitted for clarity.

the Arctic cooling. By contrast, the stratospheric winds are easterlies in the boreal summer, which inhibit the upward wave propagation (Fig. 5b3), leading to trivial changes in the Arctic stratosphere after removing the TP.

#### b. Responses and pathways in the upper level

The perturbation caused by the TP removal propagates northeastward from the TP region along the longitude of  $100^{\circ}$ – $120^{\circ}$ E to the subpolar region, enhancing the westerlies around  $60^{\circ}$ N significantly. This occurs only in wintertime. Figure 6 shows changes in atmospheric circulations, air temperature, wave activity flux and its divergence averaged over 100–200 hPa. The propagating pathways are clearly exhibited in the winter patterns of geopotential height and wind (Fig. 6a2). Wave activity flux also explicitly reveals the energy source of the enhancement of westerlies at  $60^{\circ}$ N (Fig. 6b2). The TP-forced stationary wave carries energy northeastward and diverges near  $60^{\circ}$ N, leading to an energy conversion from perturbation kinetic energy to mean kinetic energy (i.e., the enhancement of planetary-scale westerlies) (Fig. 6b2).

Changes in upper-level atmosphere circulations follow the classical theories of potential vorticity (PV) dynamics and stationary wave dynamics (Charney and Eliassen 1949; Held 1983; Son et al. 2019). First of all, in the winter pattern of atmospheric circulation changes, there is a large-scale anomalous low above the TP, accompanied by an anomalous high

downstream of the TP (Fig. 6b2). This occurs because of the PV constraint (i.e.,  $\zeta/H = \text{constant}$ , where  $\zeta$  is relative vorticity and  $H$  is the thickness of the atmosphere column). Neglecting surface friction and considering constant planetary vorticity  $f$ , removing the TP leads to a stretching of  $H$  and thus an increase of  $\zeta$  over the TP (i.e., an anomalous cyclonic circulation over the TP). The opposite occurs downstream of the TP, where the compressing  $H$  leads to a decrease of  $\zeta$  (i.e., an anomalous anticyclonic circulation). Bear in mind that in winter the planetary-scale westerlies expand southward to  $\sim 20^{\circ}$ N, so that it can be fully affected by the TP change. In contrast, the summer planetary-scale westerlies retreat northward, and easterlies dominate over most of the TP; thus, the perturbations over the TP are locally trapped (Fig. 6a3).

The wave activity flux and its divergence shown in Fig. 6b help us understand the pathways and energy conversion associated with the TP-forced stationary Rossby waves. They are calculated following the Takaya–Nakamura method (T-N flux; Takaya and Nakamura 1997, 2001). The T-N flux is the extended form of the E-P flux; it is extensively used to examine the horizontal propagation of the energy associated with the group velocity of stationary Rossby waves (Qiao and Feng 2016; White et al. 2017). The divergence of the wave activity flux represents where the wave disturbances are emitted and absorbed by the mean flows (Takaya and Nakamura 2001). The TP acts as a strong source of Rossby waves

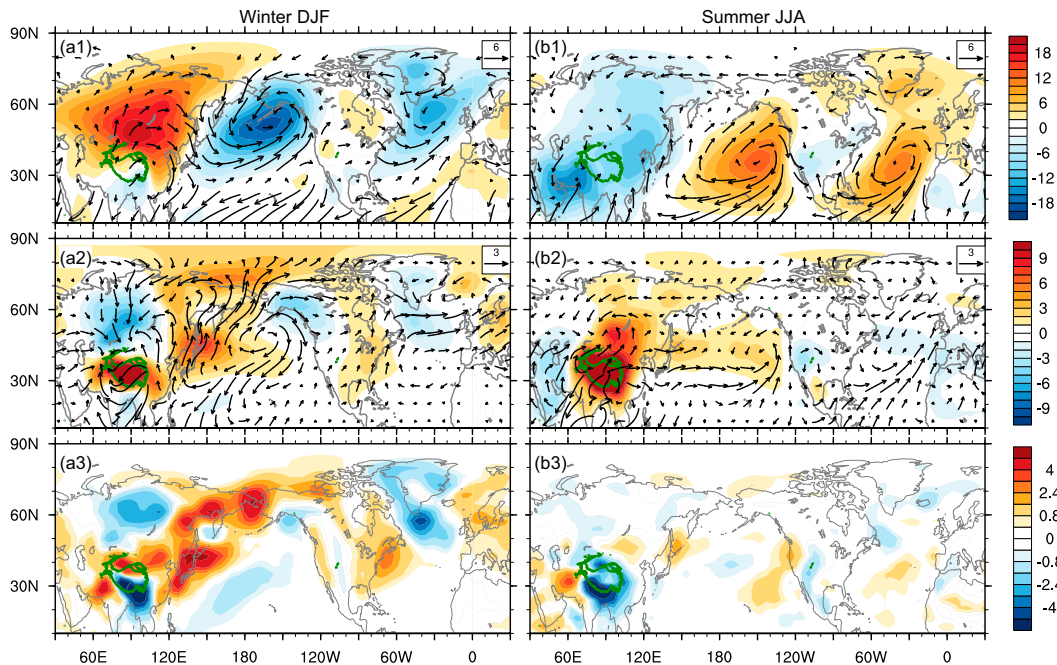


FIG. 7. (top) Surface wind (vectors;  $\text{m s}^{-1}$ ) and sea level pressure (shading; hPa) in Real. (middle) Quasi-equilibrium changes in SAT (shading;  $^{\circ}\text{C}$ ) and surface wind (vectors;  $\text{m s}^{-1}$ ) in NoTibet with respect to Real. (bottom) As in the middle panels, but for quasi-equilibrium changes in SAT advection [ $u\partial T/\partial x + v\partial T/\partial y$ ]. Results are shown for boreal (left) winter and (right) summer, averaged over years 1–100. The TP region is marked by an enclosed green contour.

(Charney and Eliassen 1949; Hoskins and Karoly 1981). Removing the TP excites the planetary stationary wave, with its energy propagating northward to northern Eurasia and eastward to the North Atlantic (Fig. 6b2). The divergence of the T-N flux in the high latitudes suggests that the wave perturbation energy is emitted and converted to mean kinetic energy, which is used to enhance the background westerlies. This energy propagation and conversion are clear in the boreal winter (Fig. 6b2). Conversely, in the boreal summer the TP-excited wave energy is locally trapped (Figs. 6a3,b3) and thus has no effect on the atmospheric circulation in the high latitudes.

In summary, for the upper-level atmospheric circulation, the TP perturbation in winter can affect the Arctic swiftly and efficiently via atmospheric processes, because the background planetary-scale westerlies favor the northeastward propagation of the wave energy (Holton and Hakim 2013). However, in the boreal summer, the planetary westerlies retreat northward and most of the TP region is controlled by the easterlies; the TP perturbation is locally trapped with negligible influence on the high latitudes.

### c. Responses and pathways in the lower level

For the lower-level atmospheric circulation, the pathways conveying the local TP warming to the Arctic are similar to those in the upper-level atmosphere. This perturbation propagation occurs also in winter only (Fig. 7). However, since the lower-level atmospheric circulation over the Asian continent is dominated by monsoon circulation, remarkably different

from the planetary circulation in the upper-level atmosphere, the mechanisms of the TP affecting the Arctic are also different.

Let us first examine the climatological atmosphere state in the NH. In winter, the Siberian high and Aleutian low dominate the Asian continent and subpolar Pacific, respectively (Fig. 7a1), and the winter northerly monsoon dominates over East China. In summer, the subtropical high dominates over the tropical and North Pacific; and the Asian continent is under low pressure (Fig. 7b1). The summer southerly monsoon dominates over East China. It implies that perturbation over the TP can hardly affect the high latitudes under the winter northerly than under the summer southerly. However, our sensitivity experiments show the opposite.

In response to the TP removal, the winter Siberian high and Aleutian low are weakened significantly, leading to strong southwesterly anomalies along the eastern coast of the Asian continent, extending from the east of the TP to the Arctic (Fig. 7a2). The strong surface warming over the TP region is thus advected eastward and northeastward by the large-scale southwesterlies (Fig. 7a3). In contrast, the impact of local warming over the TP on the Arctic is negligible in summer (Fig. 7b3), although the warming magnitude over the TP is stronger in summer than in winter (Fig. 7b2). This is because summer low pressure over the whole Asian continent (Fig. 7b1) restrains the local TP perturbation from divergence (Figs. 7b2,b3).

We emphasize that for the lower-level atmosphere, the pathways of the TP affecting the Arctic are controlled by the monsoon system. The local warming over the TP cannot propagate



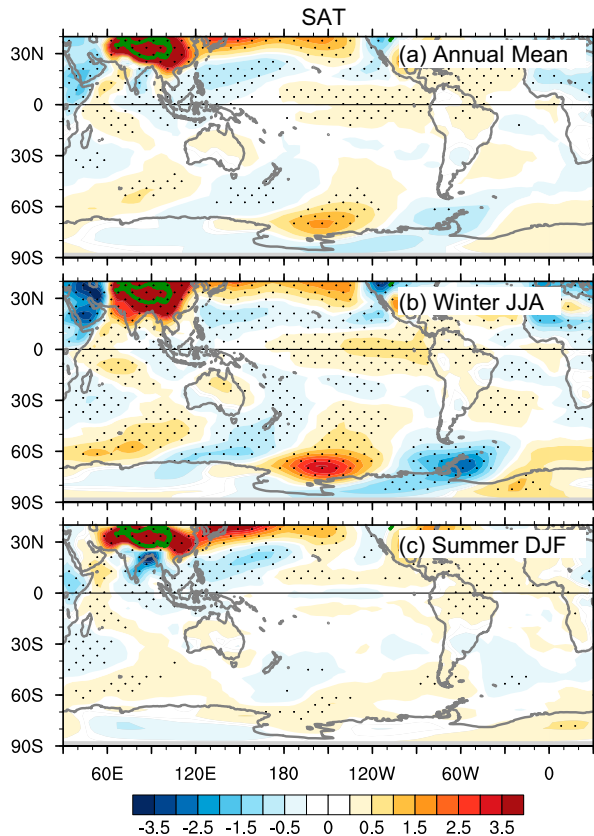


FIG. 8. Changes in SAT (shading;  $^{\circ}\text{C}$ ) in NoTibet with respect to Real, averaged over years 1–30: (a) annual mean, (b) austral winter, and (c) austral summer. In the ocean, SAT is roughly equal to SST. The TP region is marked by an enclosed green contour. Stippling represents the SAT changes are significant at the 95% confidence level based on Student's  $t$  test.

directly northward to inland Asia in winter due to the blocking of background northerlies, while it can in summer with the help of the southerlies. Therefore, the pathways in the boreal winter are eastward from the TP to the western Pacific and then northeastward to the Arctic, whereas the pathways in the boreal summer are northward to North Asia but are blocked near  $60^{\circ}\text{N}$  by anomalous easterlies.

#### 4. From the Tibetan Plateau to the Antarctic

##### a. Temperature change over the tropics and Antarctic

In response to the TP removal, a dipole-like change occurs in the tropical Indian Ocean, an El Niño-like change occurs in the tropical Pacific, and a Rossby wave-like change occurs in the Southern Ocean (Fig. 8). These changes are much stronger in the austral winter (Fig. 8b) than in the austral summer (Fig. 8c). Changes in the SH austral winter are significant at the 95% level, based on Student's  $t$  test, while they are not significant in the austral summer. For visual clarity, we do not show significance in other figures in this section. Figure 8 shows the quasi-equilibrium changes in surface air temperature (SAT)

averaged over years 1–30 after the TP is removed. The tropical Indian Ocean SST change is due to the weakening South Asian monsoon (Liu and Yin 2002; Boos and Kuang 2010; Chen et al. 2014): the weakening southerlies over the tropical Indian Ocean in the boreal summer (i.e., austral winter) lead to a weakened latent heat loss and thus SST warming there (Chen et al. 2021). The tropical Pacific SST change is due to the weakened trade wind (Wen and Yang 2020). We are particularly interested in the Rossby wave-like temperature change near the coast of the Antarctic: a cooling to the west of the Ross Sea, a warming in the west of the Amundsen Sea, and cooling over the eastern Bellingshausen Sea and Weddell Sea (Fig. 8a2). We ask the following questions: Through which pathways does the TP affect the high-latitude SH, and why is the response in austral winter much stronger than that in austral summer?

##### b. Seasonality and pathways

First of all, we stress that the most important atmospheric process in the TP affecting the Antarctic is still the stationary Rossby wave, similar to that in the NH. However, in the NH it is the TP-forced stationary wave, whereas in the SH it is the Indian Ocean SST-forced stationary wave. We want to emphasize that the tropical SST changes contribute little to the response in NH. Second, the atmosphere response in the SH is roughly barotropic, whereas that in the NH is baroclinic (Fig. 2). Finally, it is in the boreal or austral winter that the TP affects the polar region the most.

The TP-influenced pathways on the Antarctic are clearly defined by the Rossby wave train structure, which occur mainly in the austral winter (Fig. 9a). The remarkable Rossby wave with wavenumber 5 connects the tropical Indian Ocean with the Antarctic (Fig. 9a2). The wave train structure in our study is consistent with that in previous studies that investigated the teleconnection between the tropical Indo-Pacific and the Antarctic (Nuncio and Yuan 2015; Purich and England 2019; Wang et al. 2019; Gillett et al. 2022). This suggests that the tropical oceans act as a bridge in conveying the TP-forced perturbation in the NH to the SH.

A series of AGCM experiments with prescribed SST forcing further suggests that the Rossby wave train is forced by the SST change in the tropical oceans; the tropical ocean must act as a bridge in conveying the NH atmospheric perturbation to the SH, and the direct teleconnection between the TP and the Antarctic via the atmospheric bridge alone is less likely. Figure 9a shows differences from the fully coupled CESM experiments NoTibet and Real. Figure 9b shows differences from the two global SST-forced AGCM experiments (NoTibet\_SST and Real\_SST). The differences between Fig. 9a and Fig. 9b can be neglected. Figure 9c shows results from an AGCM experiment with prescribed tropical SST, namely NoTibet\_TroSST. It is seen that, except for the NH, the changes in the SH in Fig. 9c are almost identical to those in Fig. 9b. This suggests the important role of the tropical upper ocean in the Rossby wave train in the SH. The picture of the TP affecting the Antarctic is that the perturbation caused by the TP first affects the tropical ocean–atmosphere system; then, the tropical upper ocean change forces stationary wave that can propagate

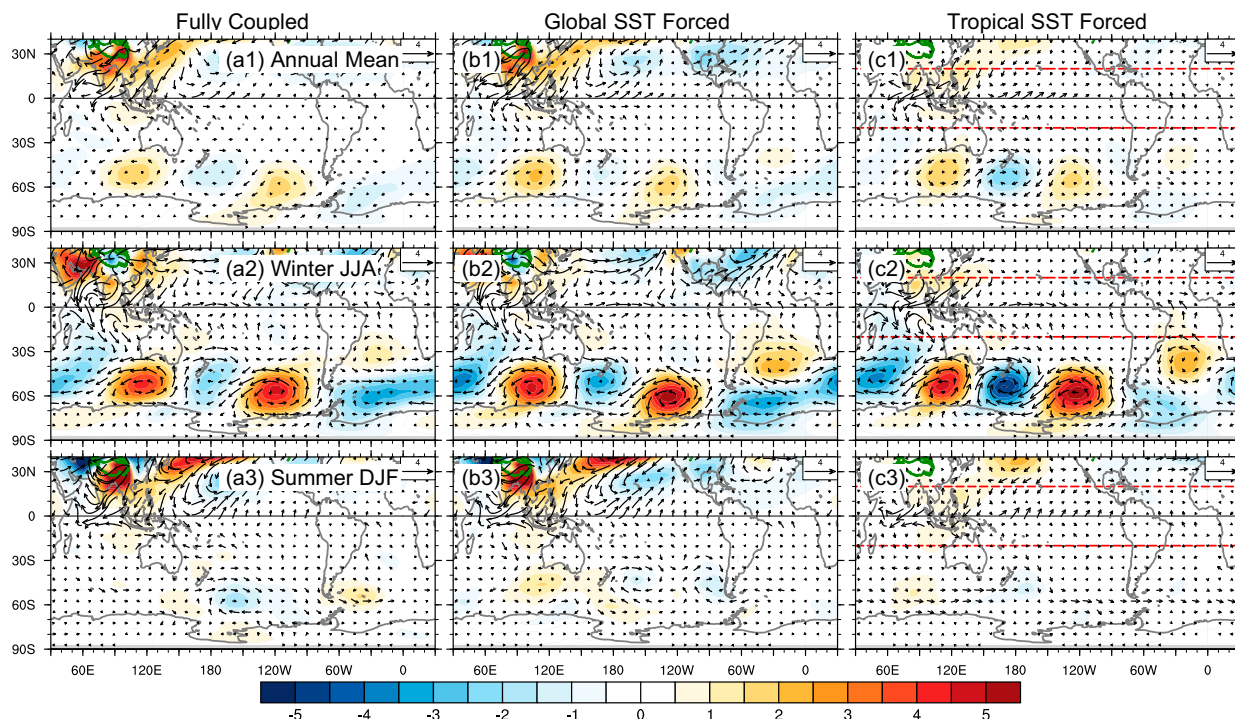


FIG. 9. Changes in surface wind (vectors;  $\text{m s}^{-1}$ ) and sea level pressure (shading; hPa) from (left) fully coupled runs (NoTibet minus Real), (center) the AGCM runs (NoTibet\_SST minus Real\_SST), and (right) the tropical-SST-forced AGCM experiments (NoTibet\_TroSST minus Real\_SST), averaged over years 1–30. All these values are obtained by subtracting their corresponding zonal mean values. The dashed red rectangle denotes the forcing region in which SST is prescribed by using that of NoTibet. Results are for the (from top to bottom) annual mean, austral winter, and austral summer, respectively. The TP region is marked by enclosed green contour.

southeastward. We suggest that the direct impact of the NH perturbation on the SH via the atmosphere bridge alone is negligible. This agrees well with previous studies (Wills and Schneider 2016, 2018; Tewari et al. 2021), which suggested the orography-forced waves cannot directly influence the other hemisphere due to the absorption of waves at the equator.

More AGCM experiments with prescribed regional SST forcing confirm that the Rossby wave train is forced by the perturbation in the tropical Indian Ocean. When forced by the dipole-like pattern in the tropical Indian Ocean, the Rossby wave train is perfectly reproduced (Fig. 10a), which occurs mainly in the austral winter (Fig. 10a2). When forced by the El Niño-like pattern in the tropical Pacific, the Rossby wave train in the SH is very weak (Fig. 10b). When forced by the SST anomaly in the tropical Atlantic, the Rossby wave train in the SH is also very weak (Fig. 10c). Besides, even the weak Rossby waves in Figs. 10b2 and 10c2 have different structures from those in Figs. 9 and 10a. This suggests that the size and sign of the forcing itself are important to the Rossby wave structure.

Removing the TP leads to weakened cross-equatorial southerlies over the Indian Ocean in the boreal summer (austral winter). This drives a positive Indian Ocean dipole (IOD)-like SST pattern in the Indo-Pacific (Chen et al. 2021). The latter excites a stationary Rossby wave, emanating from

the Indo-Pacific to the Antarctic. The wave train in the SH causes an anticyclone circulation over the Amundsen Sea and a cyclone circulation over the Weddell Sea. The anomaly northerlies over the western Amundsen Sea induce warm advection and thus SST warming. In contrast, the anomalous southerlies over the Antarctic Peninsula cause a cooling center over the Weddell Sea and eastern Bellingshausen Sea (Fig. 8).

The amplitude of Rossby wave train in the austral winter is stronger than that in the austral summer. The seasonality of the TP–Antarctica teleconnection is also due to the seasonality of the background winds in the SH (Li et al. 2015). In the austral winter, the Indian Ocean SST-forced stationary wave is located entirely within the planetary westerly belt, and the subtropical jet is strong, so the stationary Rossby waves can emanate energy from the tropical Indian Ocean to higher latitudes and excite Rossby wave train over the Southern Ocean. In the austral summer, however, the westerly belt shrinks southward, the subtropical jet is weak, and the tropics are dominated by the easterlies; thus, the Rossby wave train is not clear.

The atmospheric responses in the SH are roughly barotropic (Fig. 11 vs Fig. 9). The anomalous geopotential height and wind at 200 hPa (Fig. 11) have the same structures as those near the surface (Fig. 9), except with stronger magnitude in the upper level, which is roughly inversely proportional to the pressure.

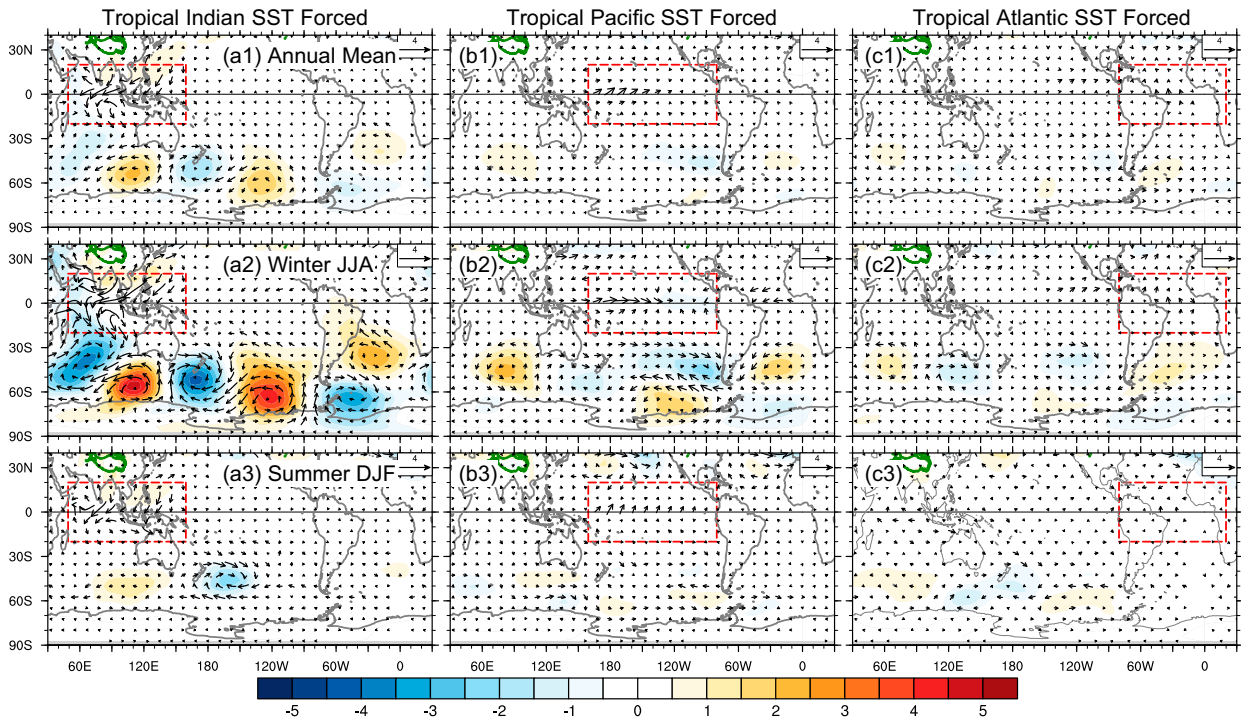


FIG. 10. As in Fig. 9, but for three different AGCM experiments: (left) tropical Indian Ocean SST-forced runs (NoTibet\_TroIO), (center) tropical Pacific SST-forced runs (NoTibet\_TroPac), and (right) tropical Atlantic SST-forced runs (NoTibet\_TroAtl). The dashed red box shows the region where the prescribed SST is applied.

The propagation direction and wavenumber of the Rossby wave train are also related to the size and sign of the forcing itself. We see that the IOD-like forcing generates the Rossby wave train with wavenumber 5 (Fig. 12a). If a uniform 1.5°C SST warming replaces the IOD-like forcing, the Rossby wave

train has wavenumbers 3 and 4 (Fig. 12b). If the forcing region doubles its size in the zonal direction, the forced Rossby wave train has wavenumbers 2 and 3 (Fig. 12c). These three AGCM experiments show clearly that the wavelength of the forced response is comparable with the size of the forcing

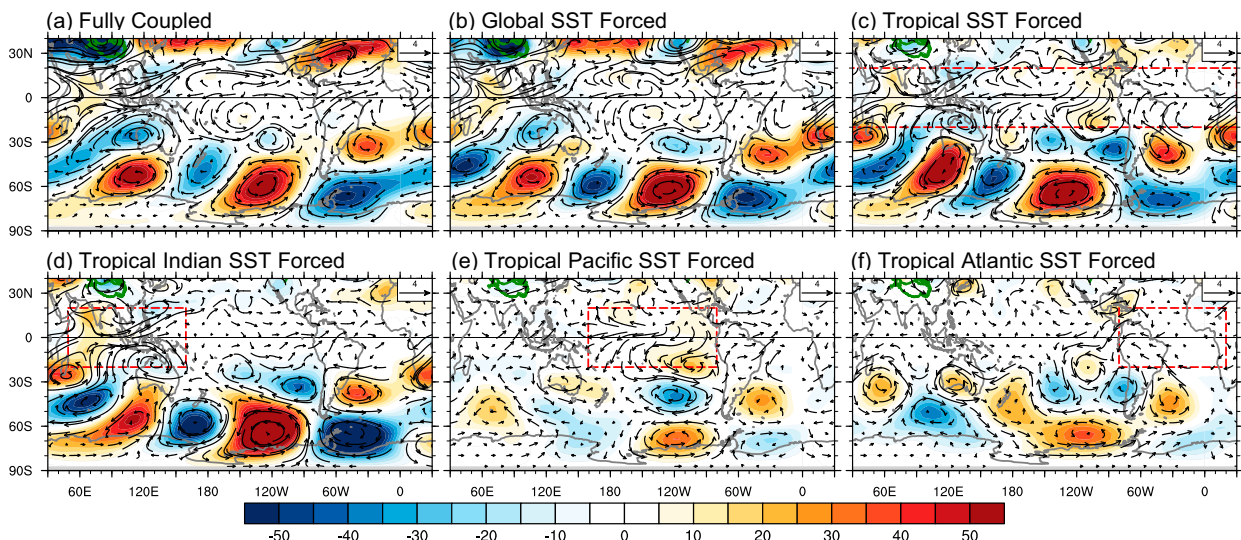


FIG. 11. (a) Changes in wind (vectors;  $m s^{-1}$ ) and eddy geopotential height (shading; m) at 200 hPa from fully coupled runs averaged over years 1–30. (b)–(f) As in (a), but for the results from AGCM runs. The dashed red box in (b)–(f) denotes the forcing region in which SST is prescribed. All values are for the austral winter.



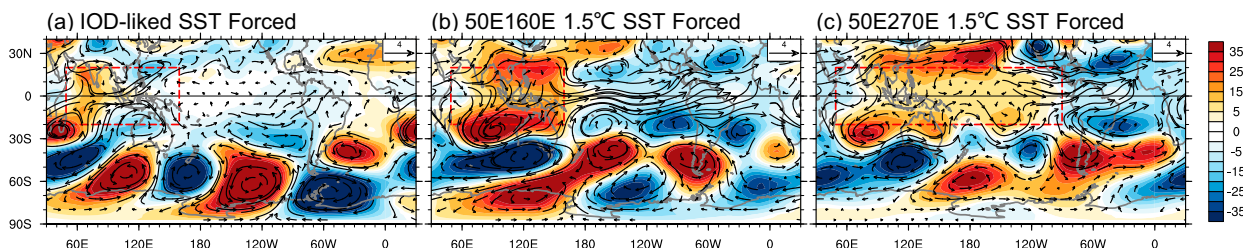


FIG. 12. Changes in wind (vectors;  $\text{m s}^{-1}$ ) and eddy geopotential height (shading; m) at 200 hPa averaged over years 1–30 in experiments forced by tropical ocean SST. (a) As in Fig. 11d, (b) for NoTibet\_TroIO\_1.5, and (c) for NoTibet\_TroIOPac\_1.5. The dashed red box denotes the forcing region. All values are for the austral winter.

itself, which can be exactly predicted by the classical stationary wave dynamics. In addition, the propagation direction of the forced waves is also determined by the ratio of zonal and meridional scales  $L_y/L_x$  of the forcing, that is,  $C_{gx}/C_{gy} \sim L_y/L_x$ , where  $C_{gx}$  and  $C_{gy}$  are the zonal and meridional group velocities, respectively. In the case of  $L_y \sim L_x$ , the wave energy propagates southeastward first and then eastward at the high latitudes, as shown in Fig. 12a. In the case of  $L_x > L_y$ , the wave energy propagates mostly southward first and then eastward at the high latitudes, as shown in Figs. 12b and 12c. These are also predictable based on the classical wave dynamics.

In summary, the TP affecting the SH is mainly bridged by the tropical Indian Ocean. Through perturbing the cross-equatorial southerlies over the Indian Ocean, the SST anomaly can generate the stationary Rossby wave that propagates southeastward to high latitudes and then generate Rossby wave train circulating the Antarctic. The SH response is roughly barotropic, with its magnitude stronger in the austral winter than in the austral summer.

## 5. Summary and discussion

Through sensitivity experiments with and without the TP, we identified the connections between the TP and polar regions. After a sudden change of the TP topography, the atmosphere adjusts immediately and reaches a quasi-equilibrium state quickly. We focus on the fast atmospheric processes in this paper. The slower ocean processes and equilibrium responses are investigated in these same experiments in our previous papers (Yang et al. 2020; Yang and Wen 2020). The TP affecting on the Arctic occurs mainly in the boreal winter, through energy propagation via topography-forced stationary waves. The TP effect on the Antarctic occurs also mainly in the austral winter, through energy propagation via SST-forced stationary waves, which are excited by the Indian Ocean SST anomaly caused by the anomalous cross-equatorial current. The latter is due to the adjustment of the South Asian summer monsoon to the TP change. In general, the change around the TP can affect the polar region significantly in winter (boreal or austral). The seasonality and pathways of the TP affecting the Arctic and Antarctic are summarized in Fig. 13.

Background mean flow is the key factor to both the seasonality and pathways of the TP affecting the Arctic. In the

boreal winter, the planetary westerly belt controls the upper atmosphere over the TP region, while the northerly monsoon controls the lower atmosphere over the Asian continent. These provide favorable conditions for the downstream propagation of the forced Rossby waves. In the upper level, the TP-forced stationary waves can carry energy directly northeastward to the Arctic (Fig. 13a). This northeastward propagation of energy owes also to the comparable zonal and meridional scales of the TP topography (Pedlosky 1987). In the lower level, the TP-forced stationary waves have to propagate eastward first, due to the blocking of the northerlies, and then go northeastward, helped by the anomalous southerlies over

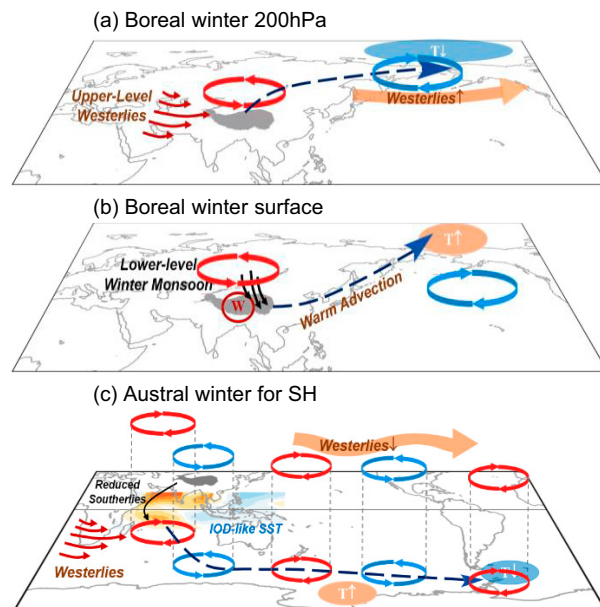


FIG. 13. Schematic diagrams showing TP–Arctic and TP–Antarctica teleconnections. (a),(b) The TP–Arctic connection in the boreal winter at 200 hPa and the surface, respectively. (c) The TP–Antarctica connection in austral winter. In (a) and (b), the gray shading denotes the TP region. The blue arrow denotes the pathways. Red arrows in (a) denote background westerlies, and black arrows in (b) denote background monsoon. The letter W represents the strong surface warming over the TP region. Shading in (c) shows the IOD-like SST pattern. Black arrows denote the reduced southerlies in the tropical Indian Ocean. Red (blue) circles represent low (high) pressure anomalies.



the region between the east coast of the Asian continent and western Pacific (Fig. 13b). In the boreal summer, the upper-level planetary westerly belt shrinks northward, and the lower-level atmosphere is dominated by the southerly monsoon; the energy of TP-forced stationary waves is more likely to be trapped locally. The baroclinic structure of background winds over the Asian continent leads to baroclinic responses in the Arctic atmosphere (Fig. 2).

The fundamental dynamics in the TP affecting the Antarctic is similar to that in the NH. In the austral winter, the TP perturbation can affect the SH via altering the cross-equatorial southerlies. Confirmed by a series of AGCM experiments, it is the SST-forced stationary waves over the Indian Ocean that carry energy southeastward, generating Rossby wave train circulating the Antarctic continent (Fig. 13c). In the austral winter, the tropical easterlies over the Indian Ocean are weak, and the SH planetary westerlies can reach lower latitudes, providing favorable conditions for the downstream propagation of the planetary waves. Different from that in the NH, the response in the SH is barotropic since the ocean–continent contrast in the SH is far less remarkable than that in the NH.

This study provides a more comprehensive picture of the TP's roles in global climate. Previous works on the TP paid much more attention to its impacts on Asia-Pacific climate than on polar regions. We trace the TP's impacts on the remote Arctic and Antarctic and identify the pathways and seasonality of the TP affecting these regions. These connections are confirmed by the Flat and OnlyTibet experiments. The atmosphere responses in the polar regions to a sudden uplift of the TP have roughly the same amplitude and opposite phase to those in NoTibet with respect to Real, suggesting that the presence of the TP can lead to a stratospheric warming (Ren et al. 2019) and surface cooling over the Arctic, a weakened (intensified) annular mode in the NH (SH), a warming over the Antarctic Peninsula, and a weakening of the Antarctic bottom water circulation. These sensitivity experiments, although highly idealized, give a useful quantitative estimate of the TP's roles in global climate, and provide an interesting viewpoint to better understanding of climate change in the polar regions.

This study can also help us understand past climate changes at the geological time scale. Paleoclimatic evidence revealed that the global climate has undergone tremendous changes since the Cenozoic, including a long cooling process marked by the development of polar ice caps and a significant reorganization of global atmospheric–oceanic circulations (Miller et al. 1991; Zachos et al. 2001). These might have some connections with the gradual uplift of the TP during the Cenozoic. Through the late Eocene to the early Oligocene, the oceanic circulations transformed from the Southern Ocean deep-water dominating mode to the present mode characterized by North Atlantic deep-water sources (Wright and Miller 1993; Davies et al. 2001; Via and Thomas 2006), consistent with our previous studies of the global thermohaline in response to the TP uplift (Yang and Wen 2020; Wen et al. 2021). However, our coupled model results showed a generally colder (warmer) climate in the NH in the absence (presence) of the TP. We demonstrate the feedback of the thermohaline

circulation change on the global climate is critical, which is absent in previous modeling studies (e.g., Ruddiman and Kutzbach 1989). The establishment of the AMOC since the gradual uplift of the TP helps establish a more northward ocean heat transport from the SH, and thus a warmer NH (colder SH). We show that the direct effect of the TP uplift may act against the global cooling and development of ice caps in the NH, but appear to favor the ice-cap formation in the SH. The global cooling since the Cenozoic derived from paleoclimatic evidence may be due to an enhanced chemical weathering rate resulting from the TP uplift or to changes in astronomical parameters.

The conclusions obtained in this paper are consistent with previous findings. For example, removing the TP can weaken the South Asian summer monsoon, consistent with the studies of Boos and Kuang (2010) and Chen et al. (2014). The teleconnection between the Indo-Pacific and the Antarctic was reported previously (Nuncio and Yuan 2015; Purich and England 2019; Wang et al. 2019; Gillett et al. 2022). Lowering the NH orography would cause the midlatitude westerlies to be more zonal (Manabe and Terpstra 1974; Ruddiman and Kutzbach 1989; Liu and Yin 2002). The weakened Siberian high and Aleutian low in winter in the absence of the TP are also consistent with previous findings (Manabe and Terpstra 1974; Hahn and Manabe 1975; Kutzbach et al. 1993; Liu and Yin 2002; Lee et al. 2013). Some previous studies determined that the Mongolian Plateau plays a vital role in the NH upper-level wintertime circulations (White et al. 2017), using AGCMs. We have performed coupled model experiments with only the TP region removed (20°–45°N, 60°–130°E), in which the response is similar to that in NoTibet, suggesting the TP's dominant role in polar region. Note that previous studies used AGCMs and we use coupled models with full ocean dynamics, which can better study the TP's role with regard to global climate.

The conclusions drawn in this paper could be affected by model bias, version, and resolution; thus, they may be model dependent. In this study, the model resolutions for atmosphere and ocean components are rather coarse. The SST simulation bias may affect the responses in the Antarctic. In addition, our experiments were carried out with fixed atmospheric CO<sub>2</sub> concentration (285 ppm) at the preindustrial level, which was lower than that during the TP uplift period (Lowenstein and Demicco 2006). The higher atmospheric CO<sub>2</sub> concentration (up to 1000 ppm) during the late Eocene should have affected the polar surface temperature change. In addition, the results obtained in our study in response to a sudden TP change may not be consistent with the climate change in response to the gradual uplift of the TP from paleoclimate viewpoint. Studies using other models with various background climate parameters are needed in the future, for a better understanding of the TP's role in shaping polar climate.

*Acknowledgments.* This work is supported by the NSF of China (91737204, 41725021, and 91937302). The experiments were performed on the supercomputers at the Chinese National Supercomputer Centre in Tianjin (Tian-He No.1).

*Data availability statement.* Datasets from this research can be obtained at <https://corp.fudan.edu.cn/Data4Paper.htm>

## REFERENCES

- An, Z., J. E. Kutzbach, W. L. Prell, and S. C. Porter, 2001: Evolution of Asian monsoons and phased uplift of the Himalaya–Tibetan Plateau since Late Miocene times. *Nature*, **411**, 62–66, <https://doi.org/10.1038/35075035>.
- Boos, W. R., and Z. Kuang, 2010: Dominant control of the South Asian monsoon by orographic insulation versus plateau heating. *Nature*, **463**, 218–222, <https://doi.org/10.1038/nature08707>.
- Budikova, D., 2009: Role of Arctic sea ice in global atmospheric circulation: A review. *Global Planet. Change*, **68**, 149–163, <https://doi.org/10.1016/j.gloplacha.2009.04.001>.
- Charney, J. G., and A. Eliassen, 1949: A numerical method for predicting the perturbations of the middle latitude westerlies. *Tellus*, **1**, 38–54, <https://doi.org/10.3402/tellusa.v1i2.8500>.
- Chen, G.-S., Z. Liu, and J. Kutzbach, 2014: Reexamining the barrier effect of the Tibetan Plateau on the South Asian summer monsoon. *Climate Past*, **10**, 1269–1275, <https://doi.org/10.5194/cp-10-1269-2014>.
- Chen, Z., Q. Wen, and H. Yang, 2021: Impact of Tibetan Plateau on North African precipitation. *Climate Dyn.*, **57**, 2767–2777, <https://doi.org/10.1007/s00382-021-05837-2>.
- Cheng, G., and T. Wu, 2007: Responses of permafrost to climate change and their environmental significance, Qinghai-Tibet Plateau. *J. Geophys. Res.*, **112**, F02S3, <https://doi.org/10.1029/2006JF000631>.
- Chiang, J. C., and Coauthors, 2015: Role of seasonal transitions and westerly jets in East Asian paleoclimate. *Quat. Sci. Rev.*, **108**, 111–129, <https://doi.org/10.1016/j.quascirev.2014.11.009>.
- Davies, R., J. Cartwright, J. Pike, and C. Line, 2001: Early Oligocene initiation of North Atlantic deep water formation. *Nature*, **410**, 917–920, <https://doi.org/10.1038/35073551>.
- Duan, A., and G. Wu, 2005: Role of the Tibetan Plateau thermal forcing in the summer climate patterns over subtropical Asia. *Climate Dyn.*, **24**, 793–807, <https://doi.org/10.1007/s00382-004-0488-8>.
- , and —, 2008: Weakening trend in the atmospheric heat source over the Tibetan Plateau during recent decades. Part I: Observations. *J. Climate*, **21**, 3149–3164, <https://doi.org/10.1175/2007JCLI1912.1>.
- Eliassen, A., and E. Palm, 1960: On the transfer of energy in stationary mountain waves. *Geophys. Publ.*, **22**, 1–23.
- Gillett, Z. E., H. H. Hendon, J. M. Arblaster, H. Lin, and D. Fuchs, 2022: On the dynamics of Indian Ocean teleconnections into the Southern Hemisphere during austral winter. *J. Atmos. Sci.*, **79**, 2453–2469, <https://doi.org/10.1175/JAS-D-21-0206.1>.
- Hahn, D. G., and S. Manabe, 1975: The role of mountains in the South Asian monsoon circulation. *J. Atmos. Sci.*, **32**, 1515–1541, [https://doi.org/10.1175/1520-0469\(1975\)032<1515:TROMIT>2.0.CO;2](https://doi.org/10.1175/1520-0469(1975)032<1515:TROMIT>2.0.CO;2).
- Harrison, T. M., P. Copeland, W. Kidd, and A. Yin, 1992: Raising Tibet. *Science*, **255**, 1663–1670, <https://doi.org/10.1126/science.255.5052.1663>.
- Held, I. M., 1983: Stationary and quasi-stationary eddies in the extratropical troposphere: Theory. *Large-Scale Dynamical Processes in the Atmosphere*. B. J. Hoskins and R. P. Pearce, Eds., Academic Press, 127–168.
- Holton, J. R., and G. J. Hakim, 2013: *An Introduction to Dynamic Meteorology*. Vol. 88, Academic Press, 553 pp.
- Hoskins, B. J., and D. J. Karoly, 1981: The steady linear response of a spherical atmosphere to thermal and orographic forcing. *J. Atmos. Sci.*, **38**, 1179–1196, [https://doi.org/10.1175/1520-0469\(1981\)038<1179:TSLROA>2.0.CO;2](https://doi.org/10.1175/1520-0469(1981)038<1179:TSLROA>2.0.CO;2).
- Hsu, H. H., and X. Liu, 2003: Relationship between the Tibetan Plateau heating and East Asian summer monsoon rainfall. *Geophys. Res. Lett.*, **30**, 2066, <https://doi.org/10.1029/2003GL017909>.
- Hunke, E. C., and W. H. Lipscomb, 2010: CICE: The Los Alamos Sea Ice Model, documentation and software user’s manual, version 4.1. Los Alamos National Laboratory Rep. LACC-06-012, 76 pp.
- Kutzbach, J., P. Guetter, W. Ruddiman, and W. Prell, 1989: Sensitivity of climate to late Cenozoic uplift in southern Asia and the American west: Numerical experiments. *J. Geophys. Res.*, **94**, 18 393–18 407, <https://doi.org/10.1029/JD094iD15p18393>.
- , W. Prell, and W. F. Ruddiman, 1993: Sensitivity of Eurasian climate to surface uplift of the Tibetan Plateau. *J. Geol.*, **101**, 177–190, <https://doi.org/10.1086/648215>.
- Lawrence, D. M., K. W. Oleson, M. G. Flanner, C. G. Fletcher, P. J. Lawrence, S. Levis, S. C. Swenson, and G. B. Bonan, 2012: The CCSM4 land simulation, 1850–2005: Assessment of surface climate and new capabilities. *J. Climate*, **25**, 2240–2260, <https://doi.org/10.1175/JCLI-D-11-00103.1>.
- Lear, C. H., H. Elderfield, and P. A. Wilson, 2000: Cenozoic deep-sea temperatures and global ice volumes from Mg/Ca in benthic foraminiferal calcite. *Science*, **287**, 269–272, <https://doi.org/10.1126/science.287.5451.269>.
- Lee, S.-S., J.-Y. Lee, K.-J. Ha, B. Wang, A. Kitoh, Y. Kajikawa, and M. Abe, 2013: Role of the Tibetan Plateau on the annual variation of mean atmospheric circulation and storm-track activity. *J. Climate*, **26**, 5270–5286, <https://doi.org/10.1175/JCLI-D-12-00213.1>.
- Li, J., and J. X. Wang, 2003: A modified zonal index and its physical sense. *Geophys. Res. Lett.*, **30**, 1632, <https://doi.org/10.1029/2003GL017441>.
- Li, X., E. P. Gerber, D. M. Holland, and C. Yoo, 2015: A Rossby wave bridge from the tropical Atlantic to West Antarctica. *J. Climate*, **28**, 2256–2273, <https://doi.org/10.1175/JCLI-D-14-00450.1>.
- Liu, X., and Z. Yin, 2002: Sensitivity of East Asian monsoon climate to the uplift of the Tibetan Plateau. *Palaeogeogr. Palaeoclimatol. Palaeoecol.*, **183**, 223–245, [https://doi.org/10.1016/S0031-0182\(01\)00488-6](https://doi.org/10.1016/S0031-0182(01)00488-6).
- Lowenstein, T. K., and R. V. Demicco, 2006: Elevated Eocene atmospheric CO<sub>2</sub> and its subsequent decline. *Science*, **313**, 1928, <https://doi.org/10.1126/science.1129555>.
- Manabe, S., and T. B. Terpstra, 1974: The effects of mountains on the general circulation of the atmosphere as identified by numerical experiments. *J. Atmos. Sci.*, **31**, 3–42, [https://doi.org/10.1175/1520-0469\(1974\)031<0003:TEOMOT>2.0.CO;2](https://doi.org/10.1175/1520-0469(1974)031<0003:TEOMOT>2.0.CO;2).
- Matsuno, T., 1971: A dynamical model of the stratospheric sudden warming. *J. Atmos. Sci.*, **28**, 1479–1494, [https://doi.org/10.1175/1520-0469\(1971\)028<1479:ADMOTS>2.0.CO;2](https://doi.org/10.1175/1520-0469(1971)028<1479:ADMOTS>2.0.CO;2).
- Miller, K. G., R. G. Fairbanks, and G. S. Mountain, 1987: Tertiary oxygen isotope synthesis, sea level history, and continental margin erosion. *Paleoceanography*, **2** (1), 1–19, <https://doi.org/10.1029/PA002i001p00001>.
- , J. D. Wright, and R. G. Fairbanks, 1991: Unlocking the ice house: Oligocene-Miocene oxygen isotopes, eustasy, and

- margin erosion. *J. Geophys. Res.*, **96**, 6829–6848, <https://doi.org/10.1029/90JB02015>.
- Molnar, P., P. England, and J. Martinod, 1993: Mantle dynamics, uplift of the Tibetan Plateau, and the Indian monsoon. *Rev. Geophys.*, **31**, 357–396, <https://doi.org/10.1029/93RG02030>.
- , W. R. Boos, and D. S. Battisti, 2010: Orographic controls on climate and paleoclimate of Asia: Thermal and mechanical roles for the Tibetan Plateau. *Annu. Rev. Earth Planet. Sci.*, **38**, 77–102, <https://doi.org/10.1146/annurev-earth-040809-152456>.
- Nuncio, M., and X. Yuan, 2015: The influence of the Indian Ocean dipole on Antarctic sea ice. *J. Climate*, **28**, 2682–2690, <https://doi.org/10.1175/JCLI-D-14-00390.1>.
- Park, S., C. S. Bretherton, and P. J. Rasch, 2014: Integrating cloud processes in the Community Atmosphere Model, version 5. *J. Climate*, **27**, 6821–6856, <https://doi.org/10.1175/JCLI-D-14-00087.1>.
- Pedlosky, J., 1987: *Geophysical Fluid Dynamics*. Springer, 710 pp., <https://doi.org/10.1007/978-1-4612-4650-3>.
- Purich, A., and M. H. England, 2019: Tropical teleconnections to Antarctic sea ice during austral spring 2016 in coupled pacemaker experiments. *Geophys. Res. Lett.*, **46**, 6848–6858, <https://doi.org/10.1029/2019GL082671>.
- Qiao, S., and G. Feng, 2016: Impact of the December North Atlantic Oscillation on the following February East Asian trough. *J. Geophys. Res. Atmos.*, **121**, 10074–10088, <https://doi.org/10.1002/2016JD025007>.
- Ramstein, G., F. Fluteau, J. Besse, and S. Jousaume, 1997: Effect of orogeny, plate motion and land–sea distribution on Eurasian climate change over the past 30 million years. *Nature*, **386**, 788–795, <https://doi.org/10.1038/386788a0>.
- Raymo, M. E., and W. F. Ruddiman, 1992: Tectonic forcing of late Cenozoic climate. *Nature*, **359**, 117–122, <https://doi.org/10.1038/359117a0>.
- , —, and P. N. Froelich, 1988: Influence of late Cenozoic mountain building on ocean geochemical cycles. *Geology*, **16**, 649–653, [https://doi.org/10.1130/0091-7613\(1988\)016<0649:IOLCMB>2.3.CO;2](https://doi.org/10.1130/0091-7613(1988)016<0649:IOLCMB>2.3.CO;2).
- Ren, R., X. Xia, and J. Rao, 2019: Topographic forcing from East Asia and North America in the northern winter stratosphere and their mutual interference. *J. Climate*, **32**, 8639–8658, <https://doi.org/10.1175/JCLI-D-19-0107.1>.
- Ruddiman, W. F., and J. E. Kutzbach, 1989: Forcing of late Cenozoic Northern Hemisphere climate by plateau uplift in southern Asia and the American West. *J. Geophys. Res.*, **94**, 18409–18427, <https://doi.org/10.1029/JD094iD15p18409>.
- Smith, R., and Coauthors, 2010: The Parallel Ocean Program (POP) reference manual ocean component of the Community Climate System Model (CCSM) and Community Earth System Model (CESM). LAUR-10-01853, 141 pp., <https://www.cesm.ucar.edu/models/cesm2/ocean/doc/sci/POPRefManual.pdf>.
- Son, J. H., K. H. Seo, and B. Wang, 2019: Dynamical control of the Tibetan Plateau on the East Asian summer monsoon. *Geophys. Res. Lett.*, **46**, 7672–7679, <https://doi.org/10.1029/2019GL083104>.
- Su, B., D. Jiang, R. Zhang, P. Sepulchre, and G. Ramstein, 2018: Difference between the North Atlantic and Pacific meridional overturning circulation in response to the uplift of the Tibetan Plateau. *Climate Past*, **14**, 751–762, <https://doi.org/10.5194/cp-14-751-2018>.
- Takaya, K., and H. Nakamura, 1997: A formulation of a wave-activity flux for stationary Rossby waves on a zonally varying basic flow. *Geophys. Res. Lett.*, **24**, 2985–2988, <https://doi.org/10.1029/97GL03094>.
- , and —, 2001: A formulation of a phase-independent wave-activity flux for stationary and migratory quasigeostrophic eddies on a zonally varying basic flow. *J. Atmos. Sci.*, **58**, 608–627, [https://doi.org/10.1175/1520-0469\(2001\)058<0608:AFOAPI>2.0.CO;2](https://doi.org/10.1175/1520-0469(2001)058<0608:AFOAPI>2.0.CO;2).
- Tewari, K., S. K. Mishra, A. Dewan, A. Anand, and I. S. Kang, 2021: Response of the atmosphere to orographic forcings: Insight from idealized simulations. *J. Atmos. Sci.*, **78**, 2691–2708, <https://doi.org/10.1175/JAS-D-19-0335.1>.
- Thompson, D. W., and J. M. Wallace, 2001: Regional climate impacts of the Northern Hemisphere annular mode. *Science*, **293**, 85–89, <https://doi.org/10.1126/science.1058958>.
- , —, and G. C. Hegerl, 2000: Annular modes in the extratropical circulation. Part II: Trends. *J. Climate*, **13**, 1018–1036, [https://doi.org/10.1175/1520-0442\(2000\)013<1018:AMITEC>2.0.CO;2](https://doi.org/10.1175/1520-0442(2000)013<1018:AMITEC>2.0.CO;2).
- Via, R. K., and D. J. Thomas, 2006: Evolution of Atlantic thermohaline circulation: Early Oligocene onset of deep-water production in the North Atlantic. *Geology*, **34**, 441–444, <https://doi.org/10.1130/G22545.1>.
- Vihma, T., 2014: Effects of Arctic sea ice decline on weather and climate: A review. *Surv. Geophys.*, **35**, 1175–1214, <https://doi.org/10.1007/s10712-014-9284-0>.
- Wang, G., H. H. Hendon, J. M. Arblaster, E.-P. Lim, S. Abhik, and P. van Rensch, 2019: Compounding tropical and stratospheric forcing of the record low Antarctic sea-ice in 2016. *Nat. Commun.*, **10**, 13, <https://doi.org/10.1038/s41467-018-07689-7>.
- Waugh, D. W., A. H. Sobel, and L. M. Polvani, 2017: What is the polar vortex and how does it influence weather? *Bull. Amer. Meteor. Soc.*, **98**, 37–44, <https://doi.org/10.1175/BAMS-D-15-00212.1>.
- Wen, Q., and H. Yang, 2020: Investigating the role of the Tibetan Plateau in the formation of Pacific meridional overturning circulation. *J. Climate*, **33**, 3603–3617, <https://doi.org/10.1175/JCLI-D-19-0206.1>.
- , C. Zhu, Z. Han, Z. Liu, and H. Yang, 2021: Can the topography of Tibetan Plateau affect the Antarctic Bottom Water? *Geophys. Res. Lett.*, **48**, e2021GL092448, <https://doi.org/10.1029/2021GL092448>.
- White, R., D. Battisti, and G. Roe, 2017: Mongolian mountains matter most: Impacts of the latitude and height of Asian orography on Pacific wintertime atmospheric circulation. *J. Climate*, **30**, 4065–4082, <https://doi.org/10.1175/JCLI-D-16-0401.1>.
- Wills, R. C., and T. Schneider, 2016: How stationary eddies shape changes in the hydrological cycle: Zonally asymmetric experiments in an idealized GCM. *J. Climate*, **29**, 3161–3179, <https://doi.org/10.1175/JCLI-D-15-0781.1>.
- , and —, 2018: Mechanisms setting the strength of orographic Rossby waves across a wide range of climates in a moist idealized GCM. *J. Climate*, **31**, 7679–7700, <https://doi.org/10.1175/JCLI-D-17-0700.1>.
- Wright, J. D., and K. G. Miller, 1993: Southern Ocean influences on late Eocene to Miocene deepwater circulation. *The Antarctic Paleoenvironment: A Perspective on Global Change*. J. P. Kennett and D. A. Warnke, Eds., Antarctic Research Series, Vol. 60, 1–25, <https://doi.org/10.1002/9781118668061.ch1>.
- Wu, G., and Coauthors, 2007: The influence of mechanical and thermal forcing by the Tibetan Plateau on Asian climate. *J. Hydrometeor.*, **8**, 770–789, <https://doi.org/10.1175/JHM609.1>.

- , Y. Liu, B. He, Q. Bao, A. Duan, and F.-F. Jin, 2012a: Thermal controls on the Asian summer monsoon. *Sci. Rep.*, **2**, 404, <https://doi.org/10.1038/srep00404>.
- , —, B. Dong, X. Liang, A. Duan, Q. Bao, and J. Yu, 2012b: Revisiting Asian monsoon formation and change associated with Tibetan Plateau forcing: I. Formation. *Climate Dyn.*, **39**, 1169–1181, <https://doi.org/10.1007/s00382-012-1334-z>.
- , and Coauthors, 2015: Tibetan Plateau climate dynamics: Recent research progress and outlook. *Natl. Sci. Rev.*, **2**, 100–116, <https://doi.org/10.1093/nsr/nwu045>.
- Yanai, M., and G. Wu, 2006: Effects of the Tibetan Plateau. *The Asian Monsoon*, B. Wang, Ed., Springer, 513–549.
- , C. Li, and Z. Song, 1992: Seasonal heating of the Tibetan Plateau and its effects on the evolution of the Asian summer monsoon. *J. Meteor. Soc. Japan*, **70**, 319–351, [https://doi.org/10.2151/jmsj1965.70.1B\\_319](https://doi.org/10.2151/jmsj1965.70.1B_319).
- Yang, H., and Q. Wen, 2020: Investigating the role of the Tibetan Plateau in the formation of Atlantic meridional overturning circulation. *J. Climate*, **33**, 3585–3601, <https://doi.org/10.1175/JCLI-D-19-0205.1>.
- , Q. Li, K. Wang, Y. Sun, and D. Sun, 2015: Decomposing the meridional heat transport in the climate system. *Climate Dyn.*, **44**, 2751–2768, <https://doi.org/10.1007/s00382-014-2380-5>.
- , X. Shen, J. Yao, and Q. Wen, 2020: Portraying the impact of the Tibetan Plateau on global climate. *J. Climate*, **33**, 3565–3583, <https://doi.org/10.1175/JCLI-D-18-0734.1>.
- Yao, T., and Coauthors, 2012: Different glacier status with atmospheric circulations in Tibetan Plateau and surroundings. *Nat. Climate Change*, **2**, 663–667, <https://doi.org/10.1038/nclimate1580>.
- Yeh, T., 1957: The wind structure and heat balance in the lower troposphere over Tibetan Plateau and its surroundings. *Acta Meteor. Sin.*, **28**, 108–121, <https://doi.org/10.11676/qxxb1957.010>.
- , and Y. Gao, 1979: *Meteorology of the Qinghai-Xizang (Tibet) Plateau*. Science Press, 278 pp.
- Zachos, J., M. Pagani, L. Sloan, E. Thomas, and K. Billups, 2001: Trends, rhythms, and aberrations in global climate 65 Ma to present. *Science*, **292**, 686–693, <https://doi.org/10.1126/science.1059412>.